Electronic Supplementary Material (ESI) for Nanoscale.
This journal is © The Royal Society of Chemistry 2018

Supplementary Information (SI)

Resolving the optical anisotropy of low-symmetry 2D materials

Wanfu Shen[a], Chunguang Hu*[a], Jin Tao[b], Jun Liu[a], Shuangqing Fan[a], Yaxu Wei[a], Chunhua An[a], Jiancui Chen[a], Sen Wu[a], Yanning Li[a], Jing Liu[a], Daihua Zhang[a], Lidong Sun[c] and Xiaotang Hu[a]

a.State Key Laboratory of Precision Measuring Technology and Instruments, Tianjin University, Weijin Road, CN-300072 Tianjin, China

b.Changchun Institute of Optics and Fine Mechanics and Physics, Chinese Academy of Science, NO.3888 Nanhu Road, CN-130033 Changchun, China

c.Institute of Experimental Physics, Johannes Kepler University Linz, A-4040 Linz, Austria

** Corresponding author:cghu@tju.edu.cn*

S1. Principle of azimuth-dependent reflectance difference microscopy (ADRDM)

The scheme of RDM setup is shown in Figure S 1. We use an off-axis parabolic mirror (OAP, Edmund, effective focal length (EFL) of 76.2mm) to convert the divergent white light emitted from deuterium and tungsten light source into a collimated beam. One non-polarizing beam splitter (BS) was applied to split incident beam into two beams. One of them was chosen as the measurement beam. The incident measurement beam goes through one polarizer, one liquid crystal variable retarder (LCVR, Thorlabs, LCC1113-A), one bjective (Nikon, 5x, NA 0.15) and the sample successively. The light reflected from sample goes back through the objective, the LCVR, the polarizer, the beam splitter, one tube lens and a band pass filter (Thorlabs, Center wavelength 600nm, FWHM 10nm) in sequence and finally is imaged on a CCD camera (Apogee, AltaU2). We drived the holders of the polarizer and the LCVR with two standard stepping motors to realize azimuth-resolved measurement by rotating polarizer and LCVR consistently. It is applied to identify the crystalline orientations of BP. The fast axis azimuthal orientations of the polarizer and the LCVR are set at 0° and 45°, respectively.

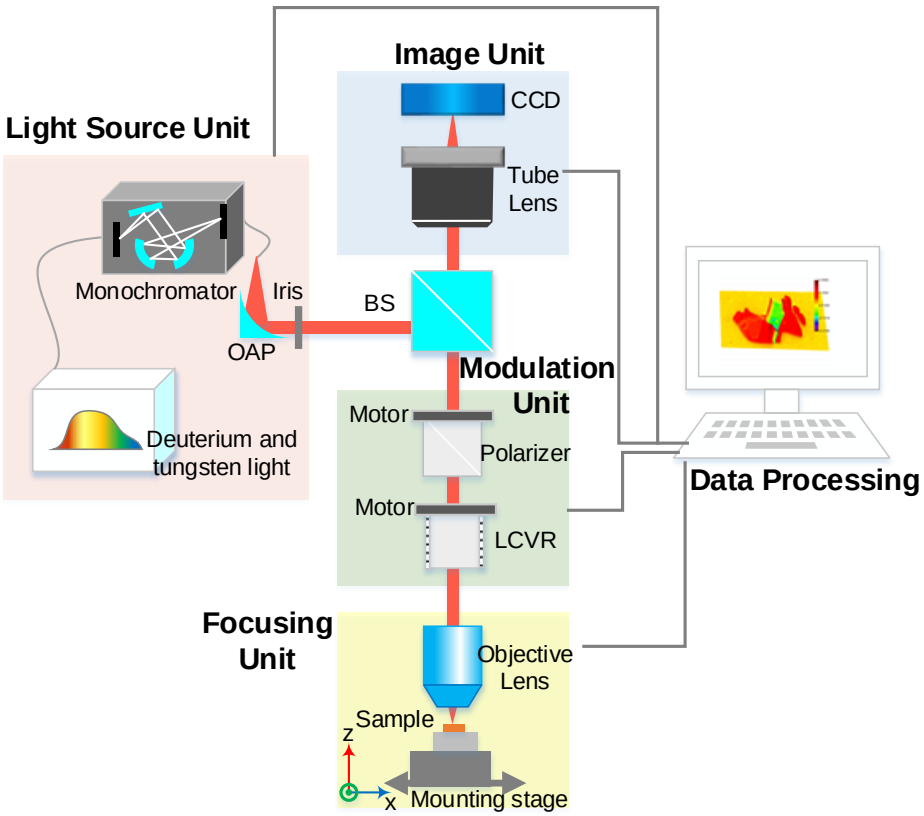

Figure S 1. Schematic diagram of the ADRDM setup. BS, beam splitter; LCVR, liquid crystal variable retarder

With the ellipsometric parameters, ψ and Δ, and the definition of $N = -\cos 2\psi$, $S = \sin 2\psi \sin \Delta$ and $C = \sin 2\psi \cos \Delta$, the $\triangle R/R$ is solved as[1]

$$\frac{\triangle R}{R} = 2\frac{R_x - R_y}{R_x + R_y} = 2N \tag{1}$$

By using Muller matrix method, the intensity I_i of each pixel of the CCD acquired at different retardations δ_i, $(i = 1, 2, \cdots, n)$ is expressed by

$$(I_1, I_2, ..., I_n) = I_0 \ \boldsymbol{M}(1 \ N \ C)^T, \tag{2}$$

where

$$\boldsymbol{M} = \begin{pmatrix} 1 + \cos^2 \delta_1 & 2\cos \delta_1 & -\sin^2 \delta_1 \\ 1 + \cos^2 \delta_2 & 2\cos \delta_2 & -\sin^2 \delta_2 \\ \vdots & \vdots & \vdots \\ 1 + \cos^2 \delta_n & 2\cos \delta_n & -\sin^2 \delta_n \end{pmatrix}. \tag{3}$$

S2. Calculation of $\Delta R/R_{za}$ of suspended BP

The $\triangle R/R_{za}$ was calculated by Eq.2-3 in the main text using three-phase Fresnel equation. For the three-phase model, we treated that the BP sheet is placed in air. The refractive indexes of BP are cited from N. Mao, et al.[2].

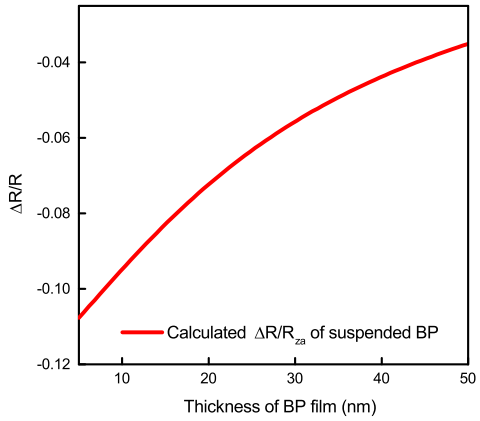

Figure S 2. Calculated $\triangle R/R_{za}$ of suspended BP flakes as a function of thickness at a wavelength of 600nm.

S3. ADRDM images of h-BN/BP/SiO_2/Si

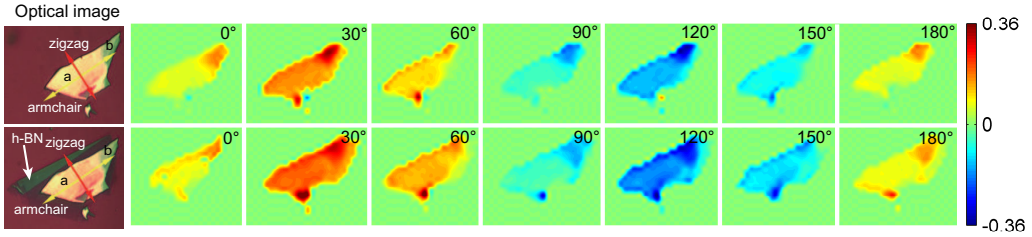

Figure S 3. Comparison of the ADRDM images of the bare and h-BN covered BP flake on Si/SiO_2 substrate at different polarization angles.

Figure S3 depicts the ADRDM images of the bare and h-BP-capped BP flake on Si/SiO_2 substrate at different polarization angles. We rotated the incident polarization angles from 0° to 180° spaced 15° in the experiment. For space saving, we only show the ADRDM images with an angular interval of 30. It is clearly seen that the isotropic h-BN cover layer only contributes a baseline offset to the $\triangle R/R$ value at each polarization angle.

S4. ADRDM images of PDMS/BP/SiO_2/Si

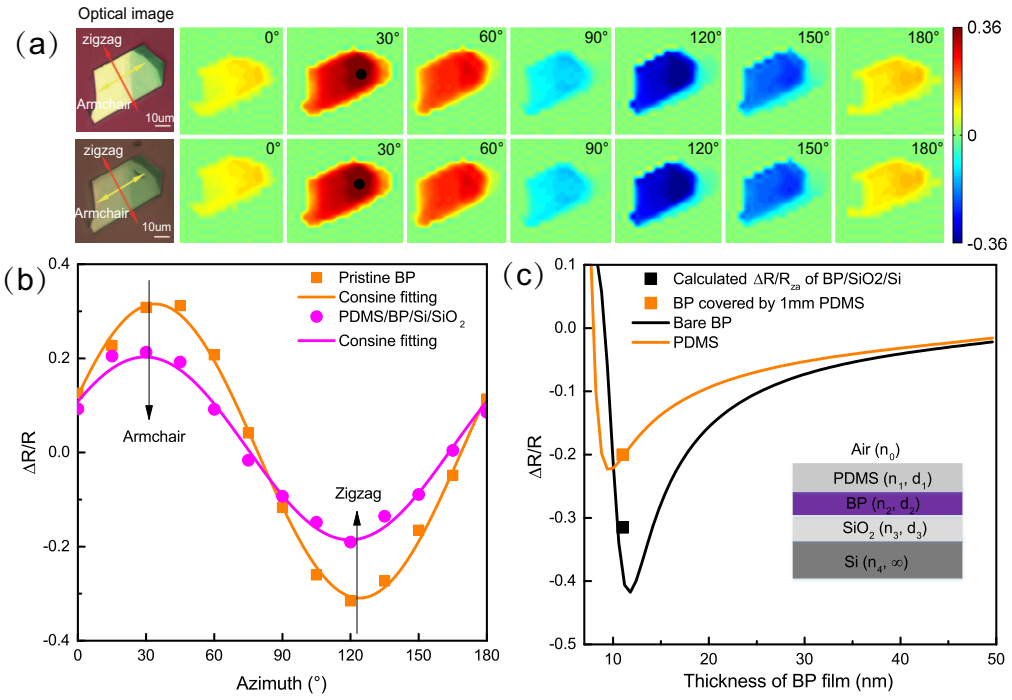

Figure S 4. (a) Comparison of the ADRDM images of the bare and PDMS covered BP flake on Si/SiO_2 at different polarization angles. (b) Plots of $\triangle R/R$ curves of bare and PDMS-capped BP. The black circulars in the RDM image of $\theta = 30°$ in (a) indicates the positions for azimuth-dependent $\triangle R/Rs$. (c) Simulated $\triangle R/R_{za}$ of BP with and without 1mm covered PDMS. The scatted squares denote the measured data.

The polydimethilsiloxane (PDMS) is widely used as intermediate material to deterministically transfer the BP flakes on various substrates during the fabrication of BP-based hterostructure[3,4]. *In situ* identifying the principle axes of BP flakes capped with PDMS film, which is relatively much thick film, will greatly benefit for deterministic fabrication of BP-based heterostructures. To this end, a BP flake was first transferred on a PDMS from a blue Nitto tape after the bulk BP was cleaved several times. We searched thin BP flakes under a normal optical microscope and then transferred the selected BP flake onto the Si/SiO_2 substrate by placing the PDMS substrate on the Si/SiO_2. The process is based on the recently developed all-dry transfer technique [3, 4]. We characterized the selected BP flake using ADRDM before and after the PDMS was peeled off, respectively. Figure S4, panel a, shows the measured ADRDM images of the bare and PDMS-capped BP as the incident polarization angles varies from 0° to 180° with an interval of 30° . This result demonstrates the capability of ADRDM as a new tool to direct visualize the distribution of

the optical anisotropy of BP flake during sample fabrication. It can benefit to select the desired BP flakes at the procedure of fabrication.

Figure S4, panel b, illustrates the plot of $\triangle R/R$ obtained from BP with and without covered PDMS versus polarization angles. The measured crystal orientations of bare and covered BP are consistent, but the amplitude of two RD curves are different because of a contribution of the PDMS layer to the total reflectivity of the sample. With a five-phase model of air/PDMS/BP/SiO_2/Si, the total scattering matrix $\boldsymbol{S}$ can be expressed by

$$\boldsymbol{S^p = I_{01}.L_1.I_{12}.L_2.I_{23}.L_3.I_{34}}. \tag{4}$$

Given the refractive index of PDMS, n, is 1.375[5], the simulation result is exhibited in Figure S 4c by orange solid line. The scattered squares present the measurement data.

S5. ADRDM images of WTe_2

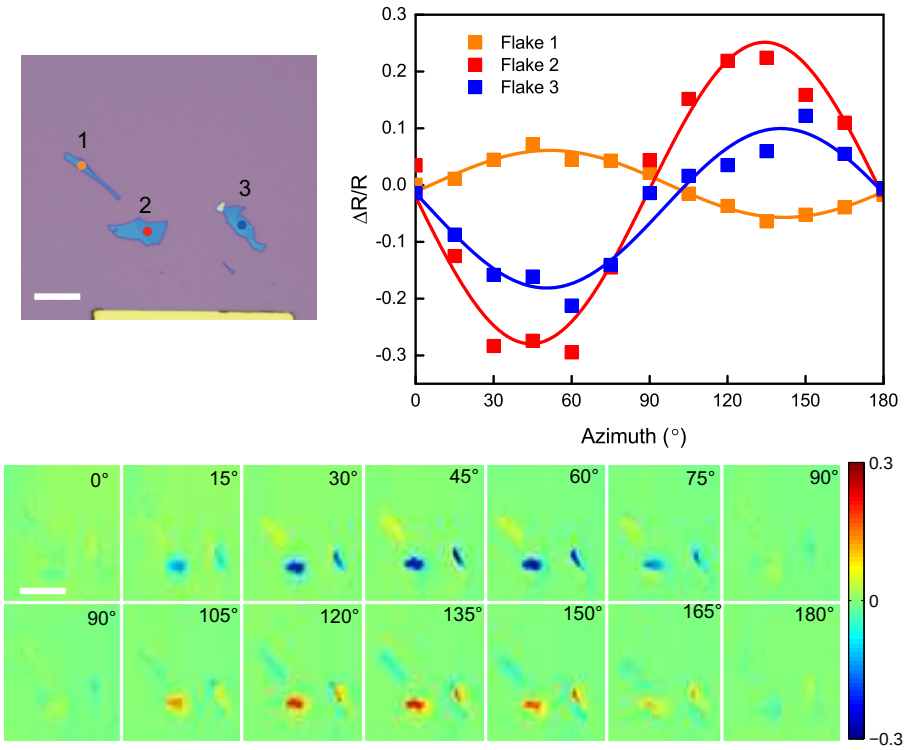

Figure S 5. (a) Optical image of typical WTe_2 on Si/SiO_2 substrate. The solid circulars indicate the positions driving $\triangle R/R$ for the plots in (b). Scale-bar: 10 µm. (b) $\triangle R/R$ versus the azimuthal angle of the incident light. (c) ADRDM images at different azimuthal angles.

References

[1] Wanfu Shen, Chunguang Hu, Shuai Li, and Xiaotang Hu. Using high numerical aperture objective lens in micro-reflectance difference spectrometer. *Applied Surface Science*, 421:535–541, 2017.

[2] Nannan Mao, Jingyi Tang, Liming Xie, Juanxia Wu, Bowen Han, Jingjing Lin, Shibin Deng, Wei Ji, Hua Xu, Kaihui Liu, Lianming Tong, and Jin Zhang. Optical anisotropy of black phosphorus in the visible regime. *J. Am. Chem. Soc*, 138(1):300–305, 2016.

[3] Andres Castellanos-Gomez, Michele Buscema, Rianda Molenaar, Vibhor Singh, Laurens Janssen, Herre SJ van der Zant, and Gary A Steele. Deterministic transfer of two-dimensional materials by all-dry viscoelastic stamping. *2D Materials*, 1(1):011002, 2014.

[4] Andres Castellanos-Gomez, Leonardo Vicarelli, Elsa Prada, Joshua O Island, KL Narasimha-Acharya, Sofya I Blanter, Dirk J Groenendijk, Michele Buscema, Gary A Steele, JV Alvarez, Henny W Zandbergen, J J Palacios, and Herre S J van der Zant. Isolation and characterization of few-layer black phosphorus. *2D Materials*, 1(2):025001, 2014.

[5] George Wypych. *Handbook of polymers*. ChemTec Publishing, 2012.